Jour. Korean Inst. Mining Geol.
Vol. 22, No. 1, p. 1 - 16, 1989

Geochemical Studies of Hydrothermal Gold Deposits, Republic of Korea : Yangpyeong – Weonju Area

So, Chil - Sup*, Choi, Sang - Hoon*, Lee, Kyeong - Yong*, and Shelton, Kevin L.**

Abstract : Electrum – galena – sphalerite mineralization of the Yangpyeong – Weonju Au – Ag area was deposited in three stages of quartz and calcite veins which fill fault breccia zones. Fluid inclusion and stable isotope data show that ore mineralization was deposited at temperatures between 260° and 180℃ from fluids with salinities between 8.9 and 2.9 equivalent weight percent NaCl. Evidence of boiling indicates pressures of <50 bars, corresponding to depths of 220 to 550 m, respectively, assuming lithostatic and hydrostatic loads. Au – Ag deposition was likely a result of boiling coupled with cooling.

Within stages I and II there is an apparent increase in $\delta^{34}S$ values of H_2S with paragenetic time ; early −1.4~2.7‰ to later 6.6~9.2‰. The progressively heavier H_2S values can be generated through isotopic re-equilibration in the ore fluid following removal of H_2S by boiling or precipitation of sulfides. Measured and calculated hydrogen and oxygen isotope values of ore – forming fluids suggest meteoric water dominance, approaching unexchanged meteoric water values. Comparison of these values with those of other Korean Au – Ag deposits reveals a relationship between depth and degree of water – rock interaction. All investigated Korean Jurassic and Cretaceous gold – silver – bearing deposits have fluids which are dominantly evolved meteoric water, but only deeper systems (≥ 1.25km) are exclusively gold – rich.

INTRODUCTION

Most gold – silver deposits in Korea are fissure – filling quartz veins intimately associated with Jurassic and Cretaceous granites (So and Shelton, 1987a, b ; So *et. al.*, 1987a, b, c). The Cretaceous granites have been shown to be higher level intrusions (<2 to 3km) than Jurassic granites (>5km, Tsusue et al., 1981). Korean deposits therefore provide an opportunity to investigate the influence of depth of emplacement on the postmagmatic evolution of hydrothermal gold – silver systems.

A geological and geochemical study of the Yangpyeong – Weonju Au – Ag area was undertaken because this area is intruded by granites of Jurassic and Cretaceous age. Within the area are a number of fissure – filling hydrothermal quartz veins which contain gold, silver, copper, lead and zinc minerals. The Samsong, Bobong, Palbo, Daenam, Boryeo, Yeosu and Jangheung mines are each located on such veins. Gold grades range from 2.5 to 200 g/metric ton, with average Au/Ag ore ratios near 1.0.

In this paper we determine the age and nature of ore mineralization in the Yangpyeong – Weonju Au – Ag area, document the physical and chemical conditions of ore deposition, and compare the area's stable isotope systematics to those of other Au – Ag deposits in the Korean Peninsula.

GEOLOGY

The Yangpyeong – Weonju Au – Ag area is located approximately 50 km ESE of Seoul within the Precambrian Gyeonggi metamorphic belt of the Korean Peninsula (Fig. 1.) The area is underlain by

* Department of Geology, Korea University, Seoul 136 – 075, Republic of Korea
** Department of Geology, University of Missouri, Columbia, Missouri 65211 USA

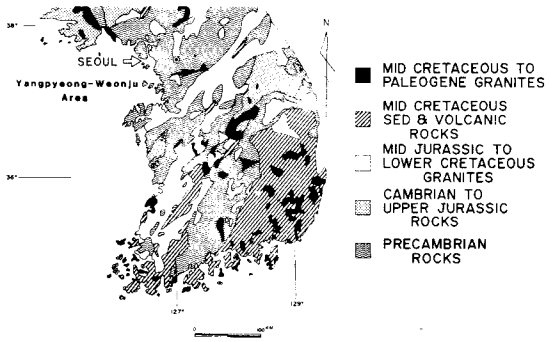

Fig. 1. Geologic map showing location of the Yangpyeong-Weonju Au-Ag area.

metasedimentary rocks of the Precambrian Gyeonggi metamorphic complex (Na, 1978, 1979a, b ; Choo et al., 1983) and is intruded by three phases of Mesozoic igneous rocks (Fig. 2).

Metamorphic rocks which crop out in the mine area consist of the Yongduri gneiss complex and the Jangrak Group, lower portions of the Gyeonggi metamorphic complex. The Yongduri gneiss complex has a general N30° to 60°E trend and is represented by banded biotite gneiss in the studied area, with locally intercalated migmatitic and porphyroblastic gneiss.

The Jangrak Group is composed of, in ascending order, quartzite and banded biotite gneiss which conformably overlie the Yongduri gneiss complex. Milky white quartzite is <300 m thick, fine- to medium-grained, has a crystalloblastic fabric and often contains biotite bands near its upper contact. Banded biotite gneiss containing small amounts of sillimanite crops out in the northern portion of the mining area and displays variable attitudes of foliation, striking N10°-30°E to N10°-20°W and dipping 30°-70°NW to 70°-80°SW. It conformably overlies the quartzite and is in contact with banded biotite gneiss of the Yongduri gneiss complex along faults. Later granitic activity obscured most primary mineral assemblages and created porphyroblastic gneiss in some areas.

Porphyroblastic and augen gneiss containing minor garnet are found mainly in the western portion of the mining area and occur as roof pendants in granite batholith. K-feldspar and plagioclase prophyroblasts (2 to 3 cm) decrease gradationally in size and amount toward the contact with banded biotite gneiss. Occasionally, porphyroblastic gneiss is transformed to augen gneiss near faults.

The metamorphic rocks have been cut by three phases of Mesozoic intrusions of basic to acidic composition : (1) the Triassic Yangpyeong igneous complex ; (2) Jurassic biotite granite ; (3) Cretaceous hornblende granite.

The Yangpyeong igneous complex consists of hornblende gabbro, diorite and porphyritic monzonite (Lee and Kim, 1974). Hornblende gabbro, containing hornblende, plagioclase (An 42 to 54) and biotite with minor microcline, augite, chlorite, epidote, apatite and magnetite, displays a coarse- to medium-grained hypidiomorphic granular texture. Augite was altered to hornblende by uralitization. Medium-grained diorite, occurring as small stocks and dikes, intrudes the hornblende granite. It is composed of plagioclase (An 25 to 34), biotite, hornblende, microcline, orthoclase, quartz and accessory apatite, zircon, rutile and chlorite. Porphyritic monzonite intrudes the hornblende gabbro and in some places contains abundant gabbro xenoliths. It is the dominant rock type in the complex and is composed of alkali-feldspar and plagioclase (An 19 to 32) phenocrysts up to 3 cm, hornblende, biotite with minor secondary chlorite.

Jurassic biotite granite contains feldspar phenocrysts from 0.5 to 2.0 cm in diameter which display micrographic and myrmekitic textures. It is composed of quartz, plagioclase (An 4 to 28), orthoclase, microcline, biotite and accessory apatite, hornblende, muscovite, zircon, allanite, sphene, magnetite, ilmenite and pyrite.

Cretaceous hornblende granite commonly shows porphyritic textures with feldspar phenocrysts from 0.5 to 1.0 cm in diameter. Its main constituents are quartz, orthoclase, hornblende, muscovite, biotite, plagioclase and accessory monazite and garnet.

Felsic and andesitic dikes, frequently porphyritic and pegmatitic, intrude all rock types along N-S-trending joints which parallel the trend of ore veins.

ORE VEINS

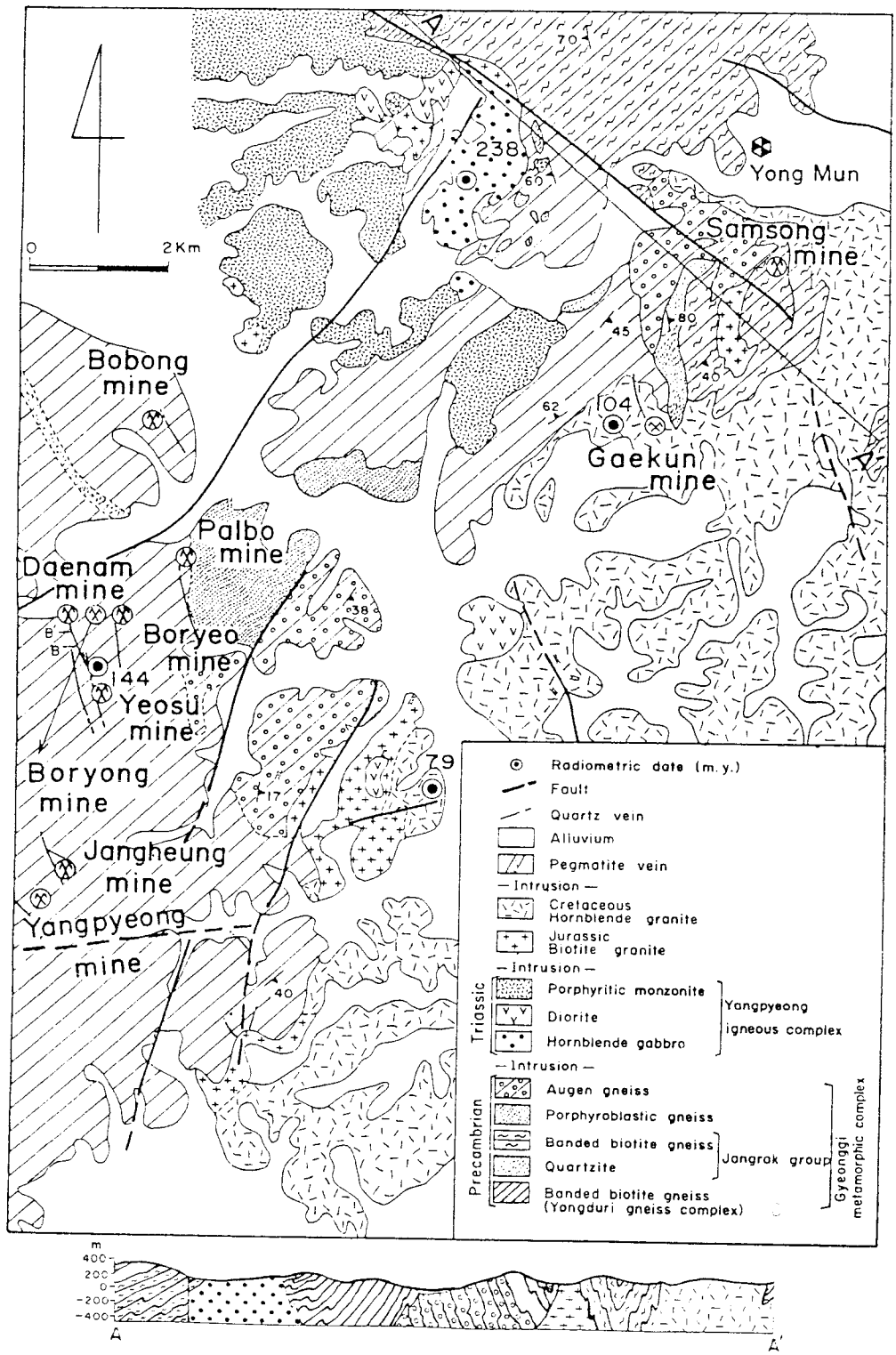

Fig. 2. Geologic map and cross-section of the Yangpyeong-Weonju Au-Ag area.

Within the mineralized area is an extensive system of subparallel gold-bearing hydrothermal quartz veins which were formed by narrow open-space filling along N-S-trending fault shear zones in Precambrian banded biotite gneiss of the Yongduri gneiss complex (Fig. 2).

Principal veins of the area are typified by those of the Daenam mine (Fig. 2), Where three small, parallel lodes follow a strongly brecciated fault zone. The gold-bearing veins strike N10° W to N-S, dip 20° to 50° SW and can be followed about 1 km along strike. Repeated pinching and swelling has led to variable vein widths(0.5 to 4.0 m) which decrease where vein dips steepen.

Mineralized veins consist chiefly of two generations of white and clear quartz with minor sulfides. Wall rock fragments are commonly contained within the ore veins, forming chambered veins where the vein thickness increases (Fig. 3). In places, wall rock fragments are highly silicified, nearly assuming the appearance of massive white quartz. Later movements in the veins are indicated by narrow clear quartz veinlets within the main brecciated massive white quartz. Massive calcite veins are found contiguous to breccia veins and infrequently occur within brecciated white quartz.

Two main gold ore shoots consisting of fine-grained electrum and pyrite occur within upper portions of the main vein of the Daenam mine (Fig.4). Wall rock adjacent to ore veins is strongly silicified and contains sericite, pyrophyllite and pyrite.

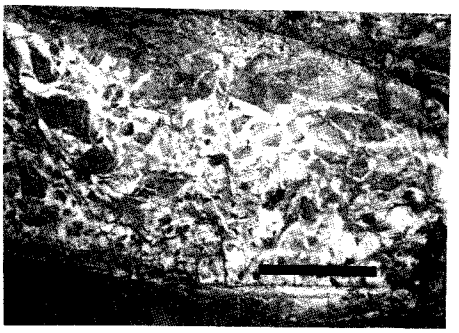

Fig. 3. Stagé I white quartz filling fault breccia zone of the Daenam mine. Scale bar is 1.0 m.

Productive veins of the Jangheung mine (Fig. 2) differ slightly from those of other mines in the area. They have thicknesses up to 0.4 m and consist of coarse-grained clear quartz with minor sulfide accumulations near vein margins. Fine-grained pyrite and alteration-derived chlorite line infrequent vugs. Wall rocks adjacent to these veins display weak argillic alteration with pyite.

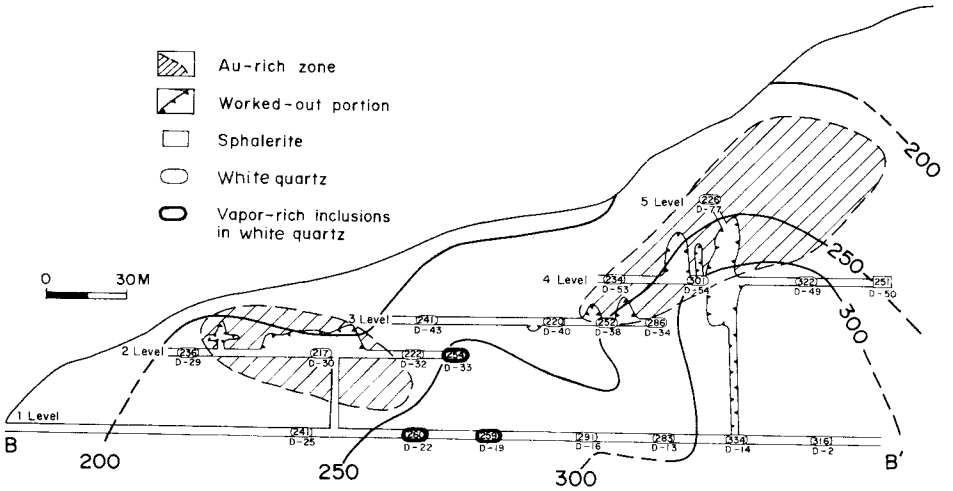

Fig. 4. Longitudinal cross-section of the Daenam mine displaying relationship of ore shoots to homogenization temperatures of primary fluid inclusions in stage I minerals.

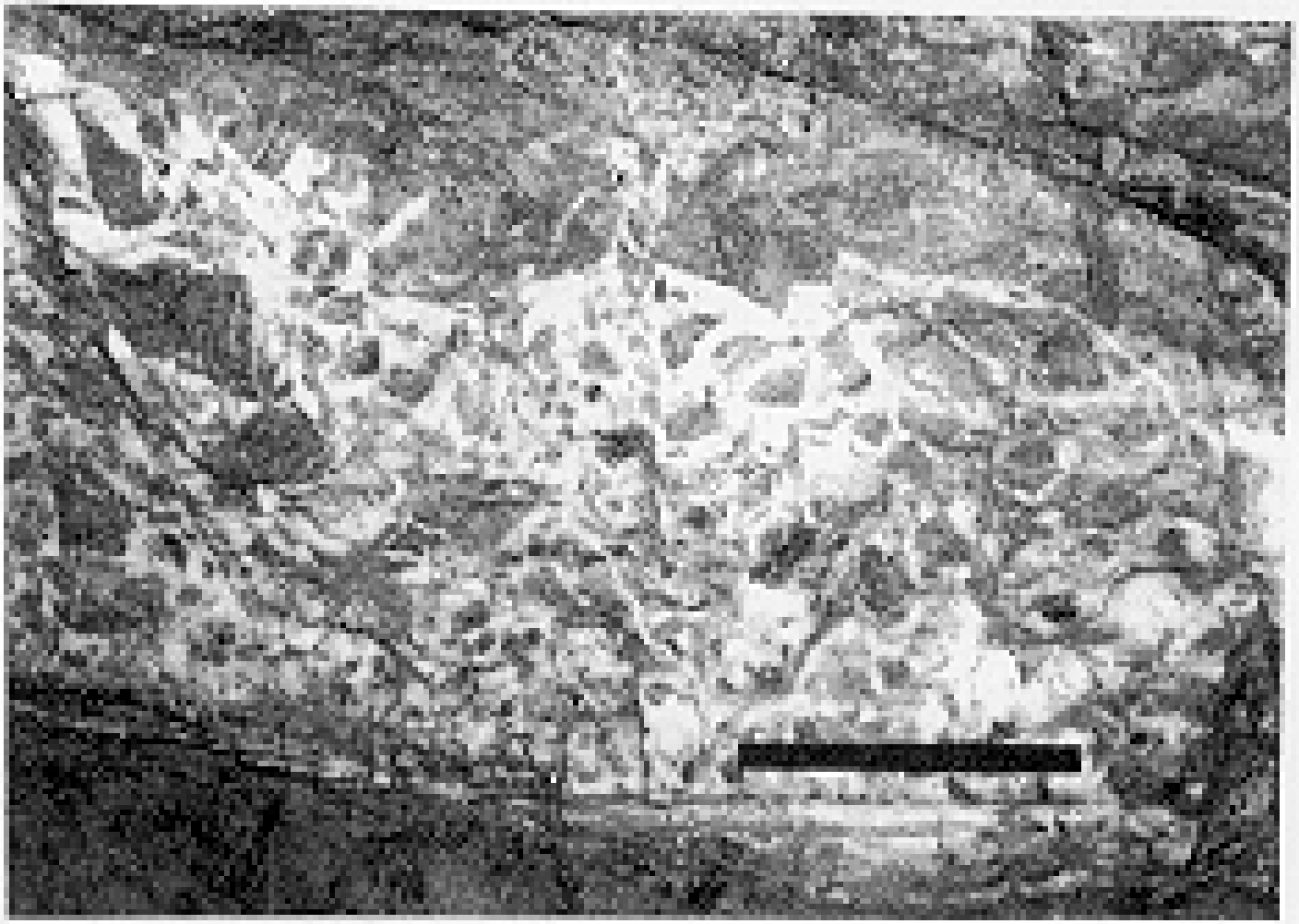

Table 1 Rb-Sr and K-Ar data of specimens from the Yangpyeong-Weonju Au-Ag area.

A. Rb-Sr data-two-point isochron.

Description	^{86}Sr ppm	^{87}Rb ppm	$^{87}Sr/^{86}Sr$	$^{87}Rb/^{86}Sr$	Isochron Parameters slope($x10^{-3}$)	intercept	Date m.y.$\pm1\sigma$
hornblende granite							
whole-rock	30.24	40.41	0.7451	8.214	1.124	0.7359	79.0±5.0
biotite	4.859	36.30	0.7372	1.186			
granodiorite							
whole-rock	52.10	63.94	0.7054	1.213	1.482	0.7036	104.3±4.4
biotite	3.66	64.89	0.7296	17.540			

B. K-Ar data.

Description	%K	Radiogenic ^{40}Ar cc/g STP $x10^{-6}$	Atmospheric ^{40}Ar%	Date m.y.$\pm1\sigma$
hornblende from Yangpyeong igneous complex	0.734	13.48	45.6	238.9±8.6
muscovite from pegmatite	6.58	38.48	3.3	144.5±5.2
sericite (kaolinite+ montmorillonite $\leq$(10%) from alteration selvage, Daenam mine	5.50	14.69	57.8	67.5±1.6

DATING OF IGNEOUS ACTIVITY AND MINERALIZATION

Dates were obtained for major igneous rock types and mineralized veins in the Yangpyeong-Weonju area using Rb-Sr and K-Ar methods. The results are presented in Table 1.

Hornblende from hornblende gabbro of the Yangpyeong igneous complex yielded a K-Ar date of 238.9±8.6 m.a., confirming a Triassic age. Muscovite from pegmatite yielded a K-Ar date of 144.5 ±5.2 m.a., suggesting a Jurassic-Cretaceous boundary age.

Hornblende granite yielded dates of 79.0±5.0 m.a. and 104.3±4.4 m.a. using a Rb-Sr two-point isochron. Sericite (containing<10% kaolinite and montmorillonite) from an alteration selvage in the Daenam mine yielded a K-Ar date of 67.5± 1.6 m.a., indicating a Late Cretaceous age for gold mineralization, believed to be associated with intrusion of the hornblende granite. This age is similar to an 88.2±3.7 m.a. age for the Okbong Au-Ag mine in the nearby Yeoju area (So and Shelton, 1987b), suggesting a regional Late Cretaceous gold metallogenic Epoch.

MINERALOGY AND PARAGENESIS

Textural relationships indicate that veins were formed in three stages (I, II and carbonate), separated by fracturing and brecciation events. Stages I and II are quartz-sulfide stages; the third stage, a

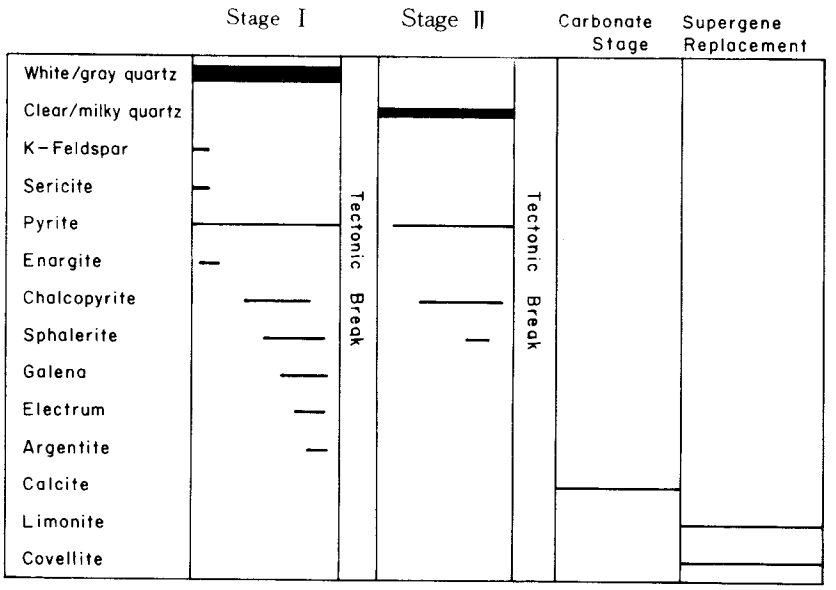

Fig. 5. Generalized paragenetic sequence of vein minerals in the Yangpyeong-Weonju Au-Ag area. Width of lines corresponds to relative abundance.

postore carbonate stage. The three stages are best displayed in main veins of the Daenam, Jangheung and Samsong mines. Generalized paragenetic sequence of vein minerals is summarized in Fig.5.

Stage I

Stage I consists mainly of white to gray quartz containing finely disseminated pyrite, chalcopyrite, galena and sphalerite, and microscopic enargite, electrum and argentite. Quartz occurs as cryptocrystalline masses and clearer drusy quartz overgrowing chlorite-rich altered wall rock fragments in breccias.

Pyrite shows weak anisotropism and is commonly penetrated and replaced by chalcopyrite. Enargite occurs rarely as small ($<3\mu m$) inclusions in early pyrite.

Dark brown, rarely yellow sphalerite containing small chalcopyrite and pyrite blebs are found as irregular masses with galena and pyrite. Sphalerite is replaced along fractures and margins by supergene covellite.

Galena occurs as anhedral grains interstitial to quartz and replaces pyrite, chalcopyrite and sphalerite along fractures and grain margins. Argentite occurs as small rounded grains in galena. Electrum (55.0 to 60.0 wt. % Au) is found associated with galena in sulfide aggregates in minute tension cracks in quartz.

Stage II

Stage II followed movements along vein strike which created narrow gouge zones in stage I veins. It consists mainly of clear to milky quartz with minor pyrite, chalcopyrite and sphalerite.

Carbonate Stage

Barren white calcite veins of variable thickness (0.5 to 4.0 cm) are developed within pre-existing veins, commonly with N20°E trends. Calcite is typically massive, but is found rarely as euhedral rhombohedral crystals.

FLUID INCLUSION STUDY

Fluid inclusions(1613 primary, 450 secondary) were examined in 55 samples of quartz, calcite and sphalerite. Gold-bearing quartz was generally unsuitable for fluid inclusion study because of its massive, fine-grained nature. Clearer drusy quartz crys-

tals proved more useful. Microthermometric measurements were made using a Leitz heating–freezing stage. Homogenization temperatures have errors of ±2.0° C. Salinity data are based on freezing point depression in the system H_2O – NaCl (Potter *et. al.*, 1978). Results of heating and freezing experiments are presented in Figures 6 through 10.

Two types of inclusions were observed, liquid–rich and vapor–rich, which range from 5 to 175μm in diameter (most 5 to 30μm) and do not contain daughter minerals. Liquid–rich inclusions are the dominant type and contain vapor bubbles comprising 10 to 40 volume percent. Vapor–rich inclusions occur only as primary inclusions, range from 10 to 40μm in diameter and contain vapor bubbles comprising 70 to 90 volume percent. Crushing tests indicate that CO_2 is present, but not in significant concentrations (<0.4 mole %).

Inclusions in Stage I

Primary inclusions in white and gray quartz homogenize from 160° to 347°C(vapor–rich inclu-

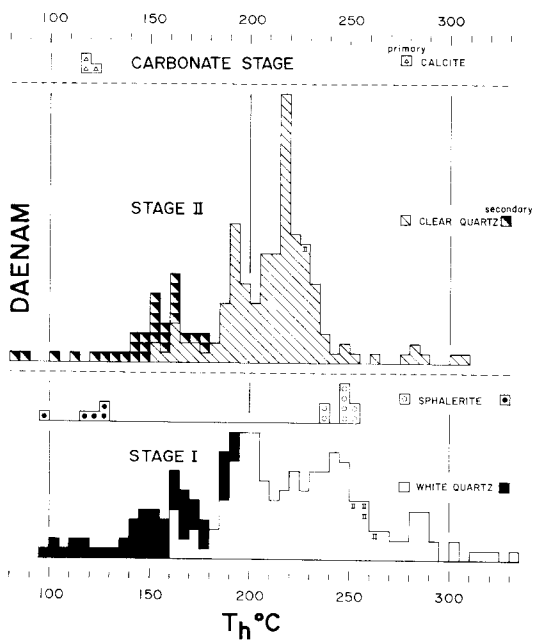

Fig. 6. Histograms of homogenization temperatures of fluid inclusions in vein minerals of the Daenam mine. II=vapor–rich inclusions.

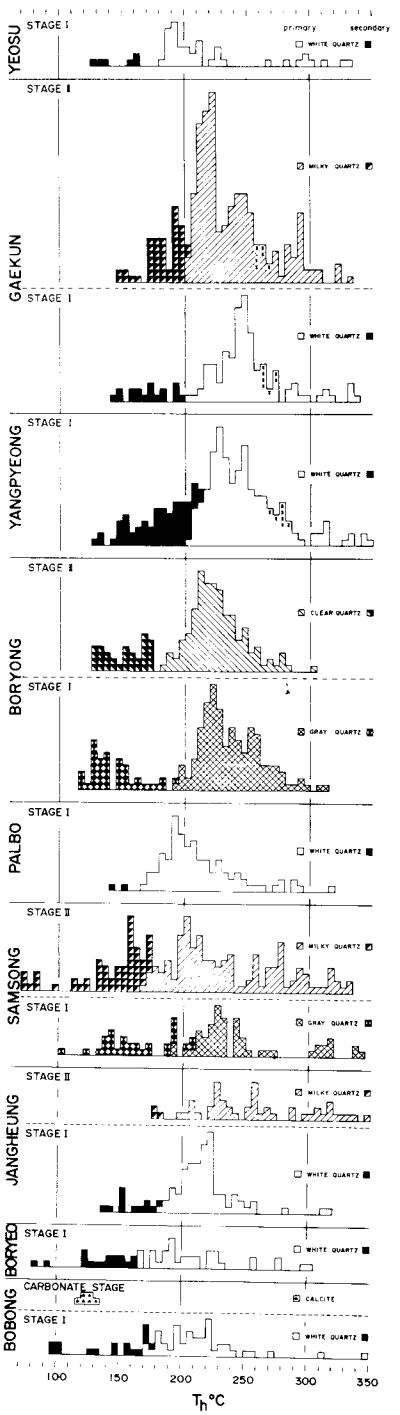

Fig. 7. Histograms of homogenization temperatures of fluid inclusions in vein minerals from the Yangpyeong–Weonju Au–Ag area.

sions 254° to 282℃, Figs. 6 and 7). Individual mines have similar ranges: Daenam (160° to 334℃); Palbo (166° to 318℃); Bobong (173° to 347℃); Yeosu (184° to 331℃); Boryeo (165° to 300℃); Jangheung (184° to 318℃); Samsong (193° to 341℃); Boryong(192° to 312℃); Yangpyeong(204° to 348℃); Gaekun(201° to 338℃). Primary liquid-rich inclusions in sphalerite homogenize from 235° to 251℃.

Salinities of primary liquid-rich inclusions in quartz range from 2.9 to 8.9 eq. wt. % NaCl (Fig. 8 and 9): Daenam (2.9 to 8.7 %); Palbo (3.1 to 8.3%); Bobong (3.2 to 8.9 %); Yeosu (3.4 to 7.6 %); Jangheung (5.1 to 8.9 %); Samsong (3.1 to 7.9 %); Yangpyeong(7.0 to 8.3%); Gaekun(6.3 to 7.3%)

Inclusions in Stage II

Primary inclusions in clear and milky quartz homogenize from 150° to 347℃ (Figs. 6 and 7): Daenam (150° to 308℃); Jangheung (195° to 347℃); Samsong (166° to 334℃); Boryong (182° to 301℃); Gaekun(200° to 334℃). Salinites of these inclusions range from 2.6 to 8.7 eq. wt.% NaCl (Figs. 8 and 9): Daenam(2.7 to 8.7%); Jangheung (6.7 to 7.3%); Samsong (2.6 to 7.2%); Gaekun(5.8 to 6.9%).

Inclusions in Carbonate Stage

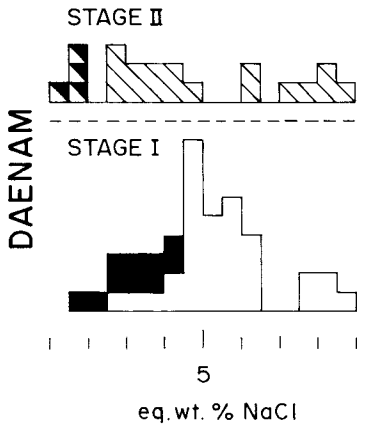

Fig. 8. Histograms of salinities of fluid inclusions in vein minerals of the Daenam mine. Symbols are the same as those in Figure 6.

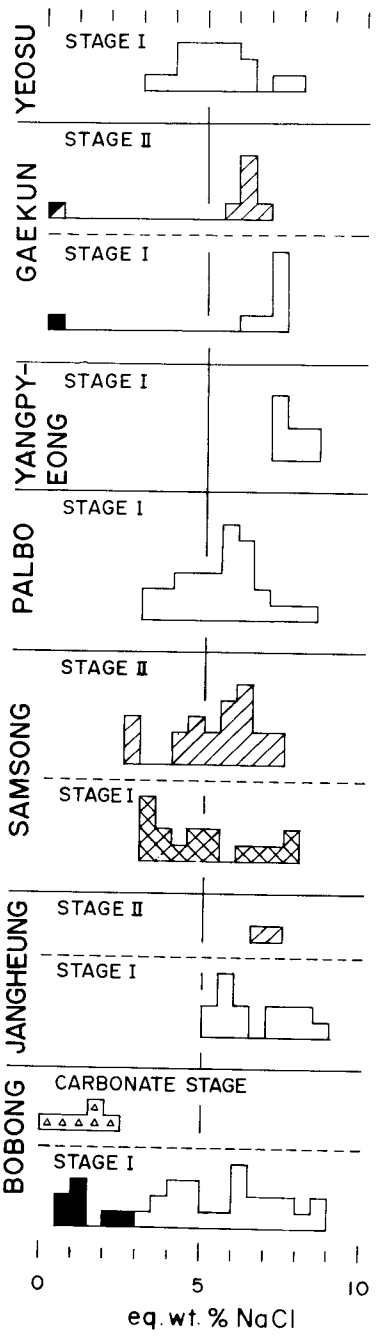

Fig. 9. Histograms of salinities of fluid inclusions in vein minerals of the Yangpyeong-Weonju Au-Ag area. Symbols are the same as in Figure 6.

Homogenization temperatures of primary liquid-rich inclusions (up to 175 μm) in white calcite range from 119° to 130°C; salinities range from 0.4 to 2.4 eq. wt. %NaCl (Figs. 6,7 and 9).

Variations in Temperature and Composition of Hydrothermal Fluids

Fluid inclusion data indicate that stages I and II evolved from initial high temperatures($\approx$350°) to later lower temperatures($\approx$150°). Each represents a separate mineralizing system which largely abated prior to the onset of the next.

The relationship between homogenization temperature and salinity in stage I and the carbonate stage (Fig. 10) suggests a complex history of boiling, cooling and dilution. During the main portion of stage I, boiling of hydrothermal fluids (δ D = -81 to -83‰) led to increases in salinity. Later cooling and dilution of ore fluids by mixing with less-evolved meteoric waters (δ D = -90‰) resulted in the linear relationship between temperature and salinity shown in Figure 10. By the advent of the carbonate stage, cooling and dilution were more pronounced, likely due to repeated fracturing events allowing more dilute meteoric waters (δ D = -109 to -111‰) into the hydrothermal system.

Homogenization temperatures of primary inclusions in stage I quartz range from 160° to 347°C (Figs. 6 and 7). Within this wide range, analysis of peaks and clusters of data within frequency diagrams has allowed us to decipher two events which are related to specific mineral assemblages (Shelton, 1983): a high-temperature group, from 350° to 260°C, thought to correspond to early quartz-K-feldspar-sericite-pyrite deposition; and a lower-temperature peak at 220°±40°C, corresponding to quartz-chalcopyrite-sphalerite-galena-electrum-argentite mineralization. The lower-temperature range is in good agreement with the temperature range for inclusions in ore-associated sphalerite(235° to 251°C) and is similar to the average range of gold deposition in many primary gold

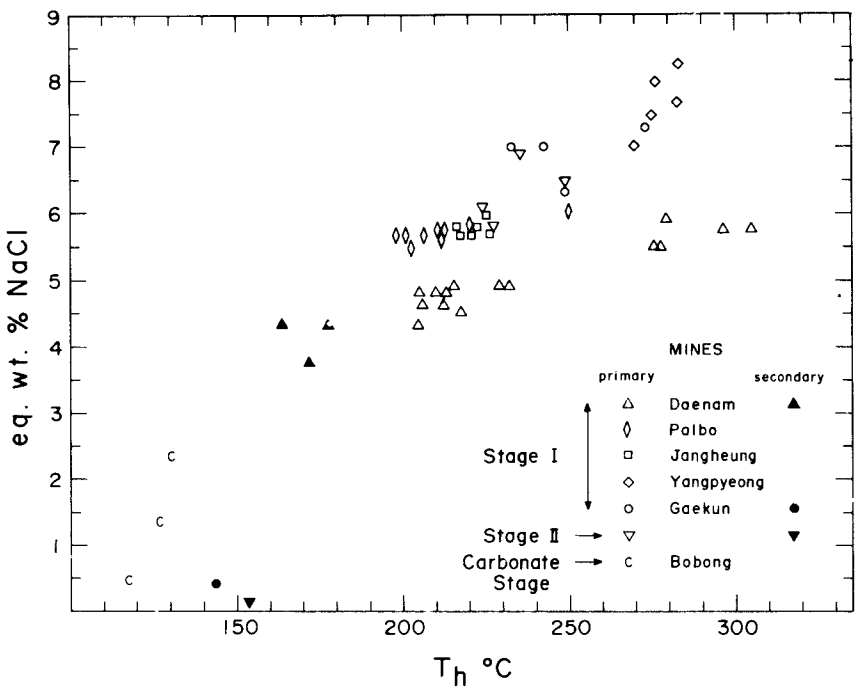

Fig. 10. Homogenization temperature versus salinity diagram for fluid inclusions in vein minerals of the Yangpyeong-Weonju Au-Ag area.

Table 2. Sulfur isotope data from the Yangpyeong- Weonju Au-Ag area.

Mine	Stage	Sample	Mineral	$\delta^{34}S$ ‰	T° C[1]	$\delta^{34}S-H_2S$ ‰[2]
Daenam	I	29	pyrite	5.5	250	4.0
		34	sphalerite	7.1	260	6.7
		40	pyrite	7.3	250	5.8
		49	pyrite	4.9	270	3.6
	II	7	pyrite	6.2	250	4.7
		10	pyrite	6.0	275	4.7
		18	pyrite	4.2	250	2.7
		20	pyrite	6.5	270	5.2
		24	pyrite	6.1	250	4.6
Bobong	I	62	pyrite	3.5	300	2.3
		64	pyrite	5.9	250	4.4
		78	pyrite	5.1	250	3.6
Yeosu	I	66	pyrite	2.7	300	1.5
		80	pyrite	7.0	250	5.5
		82	pyrite	6.9	250	5.4
		83	pyrite	7.1	250	5.6
Jangheung	I	7	sphalerite	9.6	220	9.2
			galena	6.6	220	9.2
	II	2	sphalerite	8.1	240	7.7
Palbo	I	72	sphalerite	7.0	240	6.6
			galena	6.2	240	8.6
Samsong	I	1	pyrite	6.0	250	4.5
		4	pyrite	1.7	270	0.4
	II	2	pyrite	0.4	300	−0.8
		3	pyrite	−0.2	300	−1.4
Gaekun	I	91	pyrite	3.6	300	2.4
		94	pyrite	4.9	270	3.5
		99	galena	6.9	250	9.2
			chalcopyrite	5.5	280	7.1
	II	101	pyrite	1.2	270	−0.2
		102	pyrite	2.7	290	1.4
Yangpyeong	I	110	pyrite	5.8	300	4.6
		113	pyrite	6.1	280	4.8
		115	sphalerite	8.8	234	8.4
			galena	6.0	234	8.4
Boryong	I	120	pyrite	2.0	290	0.7
		121	pyrite	4.4	270	3.0
		125	sphalerite	8.1	240	7.7
		130	galena	6.8	260	9.0
	II	140	pyrite	0.9	300	−0.3
		141	pyrite	1.5	280	0.2

[1] based on fluid inclusions in associated quartz.

[2] using isotope fractionations of Ohmoto and Rye(1979).

deposits (Nash, 1972 ; Roedder, 1984a, b). Figure 4 shows the relationship of ore shoot location to homogenization temperatures of primary fluid inclusions in stage I vein minerals of the Daenam mine. Ore is preferentially localized between the 250° and 200°C isotherms.

Pressure Considerations and Significance of Boiling

Liquid – and vapor – rich inclusions in stage I quartz homogenize at the same temperatures over the range 254° to 282°C, indicating boiling. The wide range of salinities (2.9 to 8.9 eq. wt.% NaCl) of stage I ore fluids, compared to those of most gold deposits, suggests boiling occurred throughout stage I ore deposition. Data for the system H_2O – NaCl (Sourirajan and Kennedy, 1962 ; Haas, 1971), combined with temperature and salinity data for these inclusions, indicate pressures of <50 bars. These pressures correspond to maximum depths of about 220 and 550 m, respectively, assuming lithostatic and hydrostatic loads.

Boiling in hydrothermal systems can result in abrupt chemical changes (e.g. pH, oxygen fugacity, ΣH_2S, ΣCO_2) in the liquid phase (Drummond and Ohomto, 1985). These changes favor deposition of precious metals through destabilization of metal complexes, such as $Au(HS)^{-2}$ and $AgCl^{-2}$(Seward, 1984 ; Cole and Drummond, 1986). We interpret gold deposition in the Yangpyeong – Weonju area to be a result of boiling coupled wth declining temperatures.

STABLE ISOTOPE STUDIES

Recent studies have demonstrated the usefulness of stable isotopes in elucidating the origin and history of hydrothermal fluids and their constituents in vein – type gold deposits. In this study we measured the C, O, H and S isotope compositions of quartz, clacite, sulfides and fluid inclusion waters. Standard techniques for extraction and analysis were used (McCrea, 1950 ; Grinenko, 1962 ; Roedder *et al.*, 1963 ; Hall and Friedman, 1963 ; Rye, 1966). Data are reported in standard δ notation relative to the PDB standard for C, SMOW for O and H, and CDT for S. The analytical error is approximately ± 0.1‰ for C, O and S ; ±2‰ for H(Tables 2 and 3).

Sulfur Isotope Study

Analyses were performed on 41 hand – picked sulfides from various mines of the area (Table 2). Stage I pyrite has $\delta^{34}S$ values of 1.7 to 7.3‰ ; stage I chalcopyrite, 5.5‰ ; stage I sphalerite, 7.0 to 9.6‰ ; galena, 6.2 to 6.6‰ ; stage II pyrite, −0.2 to 6.5‰ ; stage II sphalerite, 8.1‰. Two sphalerite – galena pair with a texture suggesting coprecipitation of the phases has a $\Delta^{34}S$ value of 2.8 and 3.0‰, yielding a temperature of 234° and 218° ±33°C (Ohmoto and Rye, 1979), in good agreement with homogenization temperatures of primary inclusions in sphalerite

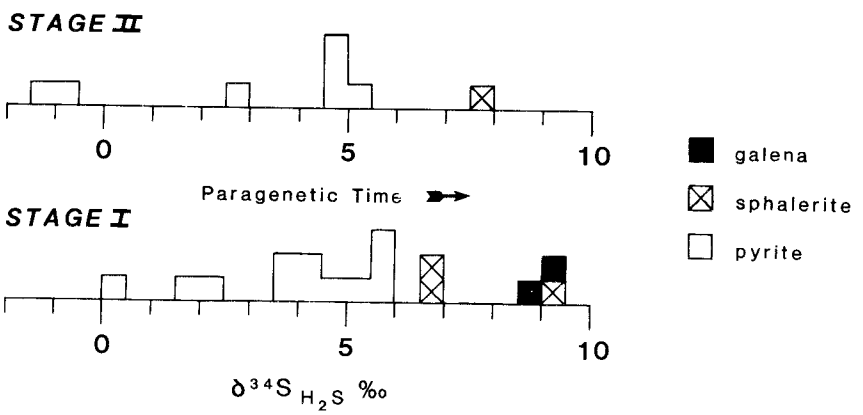

Fig. 11. Sulfur isotope compositions of H_2S during stages I and II. See Table 2 for details.

(235° to 251°C) and those in ore-associated white quartz (220°±40°C; Figs. 6 and 7).

Assuming depositional temperatures of 300° to 250°C for stage I and II pyrite and stage I chalcopyrite and 260° to 220°C for sphalerite and galena (based on fluid inclusion and paragenetic constraints), calculated $\delta^{34}S$ values of H_2S during stage I are 0.4 to 9.2‰; those for stage II, −1.4 to 7.7‰(Table 2; Fig.11). Within stages I and II there is an apparent increase in $\delta^{34}S$ values of H_2S with paragenetic time: early pyrite, −1.4 to 2.7‰; later pyrite, 3.6 to 5.8‰; sphalerite and galena, 6.6 to 9.2‰.

Three possible explanations for this phenomenon are: (1) gradual addition of sulfur from an isotopically heavy source (possibly wall rock sulfur); (2) an original isotopically heavy sulfur source (at least 9.0‰) with a increasing H_2S/sulfate ratio (reduction of sulfur); (3) isotopic re-equilibration in the ore fluid following removal of H_2S by boiling or precipitation of sulfides (reservoir effect). In case (1), heavy sulfur must be added in the same proportion at the same point in the parageneses of stages I and II. This seems unlikely. There is no mineralogical evidence that fugacity of oxygen decreased as required by case (2). We therefore prefer case (3).

Assuming an initial $\delta^{34}S_{\Sigma S}$ value of 9.0‰, in order for the $\delta^{34}S$ value of H_2S during early pyrite deposition (300°C) to be −1.0‰, the H_2S/sulfate ratio of the fluid must have been ≈ 3 : 2 (using a $\triangle^{34}S$ sulfate-H_2S value of 25‰; Sakai, 1968). Drummond and Ohmoto (1985) have shown that with only 5% boiling at 300°C, significant changes in ΣH_2S occur. If 80% of the fluids H_2S were lost during boiling, the remaining liquid would have a new H_2S/sulfate ratio of 3 : 10 with a $\delta^{34}S_{\Sigma S}$ value of 18.2‰. If rocks originally controlling the chemistry of the hydrothermal fluid were able to buffer the fluids fugacity of oxygen, then the fluids H_2S/sulfate ratio would return to a value of 3 : 2. This would result in H_2S with a $\delta^{34}S$ value of +8.2‰.Thus, progressively heavier H_2S values can be generated through boiling, loss of H_2S and isotopic re-equilibration in the fluid. Such a process could have occurred in stages I and II, and led to the measured increase in $\delta^{34}S$ values of H_2S with paragenetic time.

Table 3. C, O and H isotope data for minerals and inclusion waters from the Yangpyeong-Weonju Au-Ag area.

Mine	Stage	Sample	Mineral	$\delta^{13}C$ ‰	$\delta^{18}O$ ‰	T°C[1]	$\delta^{18}O$water ‰[2]	δDwater ‰
Daenam	I	4	quartz		1.4	310	− 5.7	− 81
		22	quartz		−2.9	235	−13.1	
		34	quartz		1.5	305	− 5.7	− 83
		54	quartz		−3.7	265	−12.5	− 90
	II	7	quartz		2.6	250	− 6.8	− 82
		20	quartz		2.7	305	− 4.5	− 84
	Carbonate	26	calcite	−5.7	7.8	120	− 7.4	−109
		33	calcite	−4.6	8.6	120	− 6.6	−111
Gaekun	I	90	quartz		0.5	300	− 6.0	− 85
		99	quartz		1.1	305	− 5.2	− 89
Samsong	Carbonate	6	calcite	−4.6	−0.5	120	−15.7	
Bobong	Carbonate	63	calcite	−3.4	10.6	130	− 3.8	
Yang-pyeong	Carbonate	116	calcite	−4.0	2.5	125	−12.1	−110

[1] based on fluid inclusion temperatures and paragenetic constraints.

[2] using fractionation equations of Clayton *et al.* (1972) and O'Neil *et al.* (1969).

Oxygen and Carbon Isotope Study

The $\delta^{18}O$ values of six quartz samples from the Daenam mine are: stage I, −3.7 to 1.5‰; stage II, 2.6 to 2.7‰(Table 3). Calculated $\delta^{18}O_{water}$ values, using the fractionation equation of Clayton *et. al.* (1972), are: stage I, −5.7 to −13.1‰; stage II, −4.5 to −6.8‰. The $\delta^{18}O$ values of two stage I quartz samples from the Gaekun mine are 0.5 to 1.1‰(Table 3). Calculated $\delta^{18}O_{water}$ values are −6.0 to −5.2‰.

The $\delta^{18}O$ values of five carbonate stage calcites from the Daenam, Yangpyeong, Bobong and Samsong mines are −0.5 to 10.6‰. Their $\delta^{13}C$ values are −3.4 to −5.7‰. Calculated $\delta^{18}O_{water}$ values, using the fractionation equation of O'Neil et al. (1969), are −3.8 to −15.7‰(Table 3).

Hydrogen Isotope Study

Inclusion waters were extracted from seven quartz and three calcite samples. Their δD values are: stage I, −81 to −90‰; stage II −82 to −84‰; carbonate stage, −109 to −111‰(Table 3).

INTERPRETATION OF ISOTOPE RESULTS

The measured range of δD values for fluids from shallow (<1.25 km), Cretaceous Au−Ag−bearing deposits in Korea is −81 to −143‰(So and Shelton, 1987 a, b; So *et al.*, 1987 a, b, c; So and Shelton, unpublished data) and is assumed to represent the range of paleometeoric water compositions in Korea at the time of mineralization. Figure 12 shows the measured and calculated fluid compositions of the Yangpyeong−Weonju Au−Ag area (mostly Daenam mine) on a conventional H vs. O isotope diagram. The range of these data is consis-

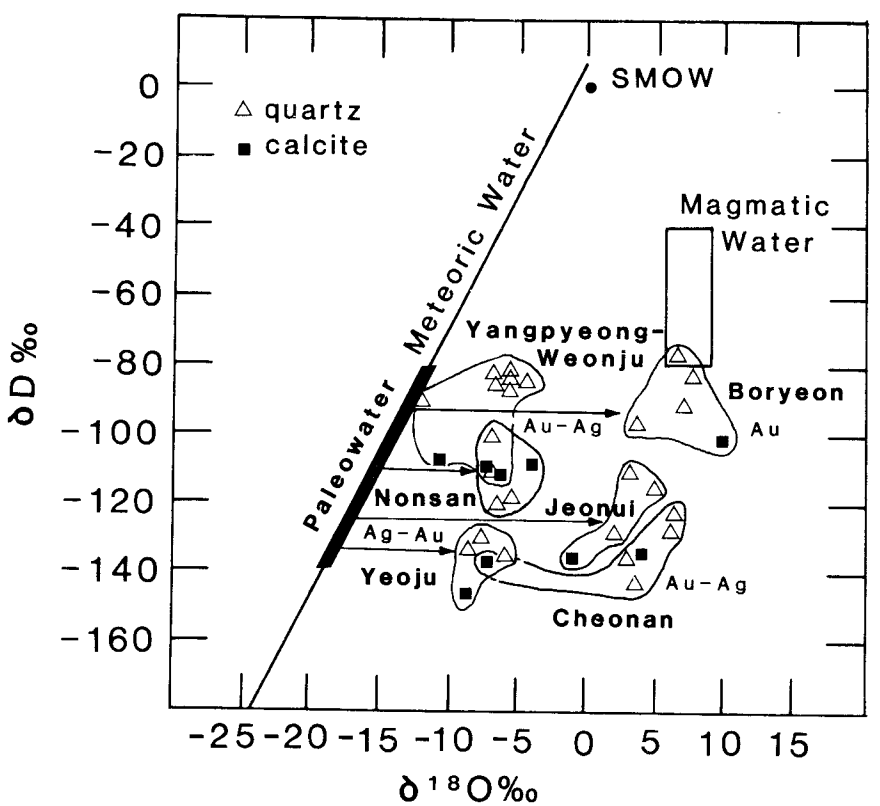

Fig. 12. Hydrogen versus oxygen isotope diagram displaying isotope systematics of fluids in Korean Au−Ag−bearing hydrothermal systems.

tent with meteoric water dominance as fluid compositions approach those of local, unexchanged meteoric waters. Significant meteoric water involvement is not surprising in the relatively shallow (< 550 m) Au-Ag systems.

For comparison, data from other Cretaceous and Jurassic Au-Ag deposits in Korea are shown in Figure 12 (So and Shelton, 1987a, b; So *et al.*, 1987a, b, c; Shelton and So, unpublished data). All of the data display various degrees of ^{18}O-enrichment relative to meteoric water, produced by isotope exchange with hot igneous rocks, the classic ^{18}O-shift (Taylor, 1974).

Data from the Jurassic Boryeon Au mine, a deeper (≈2.5 km), gold-rich hydrothermal system, differ markedly from those of other areas. Boryeon values are more enriched in ^{18}O relative to local meteoric water, indicating a higher degree of igneous rock interaction. Data from the Yangpyeong-Weonju area are most similar to those of the Cretaceous Jeonui mine and Nonsan area, shallow (<700 m) Au-Ag hydrothermal systems. Data from the Yeoju and Cheonan Au-Ag areas (≈1.25 km deep), are between those of the other areas. This suggests a relationship between depth and degree of water-rock interaction in Korean deposits. All of these gold-silver-bearing deposits have fluids which are dominantly evolved meteoric waters, but only deeper systems with higher degrees of igneous rock interaction are exclusively gold-rich.

ACKNOWLEDGEMENTS

This research was supported by grants from the Korea Science & Engineering Foundation (to So) and the U.S.-Republic of Korea Cooperative Science Program of the National Science Foundation (INT 8517627 to K. L. Shelton). Stable isotope analyses were performed in the laboratories of D. M. Rye, Yale University.

REFERENCES

Choo, S.H., Kim, D.H., Jae, W.M. (1983) Geochronological study on Gyeonggi massif in Korea peninsula by the Rb-Sr method. Jour. Korean Nuclear Soc. 15: p. 23-32.

Clayton, R.N., ONeil, J.R., Mayeda, T. (1972) Oxygen isotope exchange between quartz and water. Jour. Geophys. Research 77: p. 3035-3067.

Cole, D.R., Drummond, S.E. (1986) The effect of transport and boiling on Ag/Au ratios in hydrothermal solutions: A preliminary assessment and possible implications for the formation of epithermal precious-metal ore deposits. Jour. Geochem. Explor. 25: p.45-79.

Drummond, S.E., Ohmoto, H. (1985) Chemical evolution and mineral deposition in boiling hydrothermal systems. Econ. Geol. 80: p.126-147.

Grinenko, V.A. (1962) Preparation of sulfur dioxide for isotopic analysis. Zeitz. Neorgan. Khimii 7: p. 2478-2483.

Haas, J.L. Jr. (1971) The effect of salinity on the maximum thermal gradient of a hydrothermal system at hydrostatic pressure. Econ. Geol. 66: p.940-946.

Hall, W.E., Friedman, I. (1963) Compositions of fluid inclusions, Cave-in-Rock fluorite district, Illinois, and Upper Mississippi Valley zinc-lead district. Econ. Geol. 58: p.886-911.

Lee, D.S., Kim, Y.J. (1974) Petrology and petrochemistry of the Yangpyeong ingeous complex. Mining Geol. (Korea) 7: p. 123-138.

McCrea, J.M. (1950) The isotope chemistry of carbonates and a paleotemperature scale. Jour. Chem. Phys. 18: p. 849-857.

Na, K.C. (1978) Regional metamorphism in the Gyeonggi massif with comparative studies on the Yeoncheon and Ogcheon metamorphic belts (I) (On the general geology and petrography of Gyeonggi massif). Jour. Geol. Soc. Korea 14: p. 195-211.

Na, K.C. (1979a) Regional metamorphism in Gyeonggi massif with comparative studies between Yeoncheon and Ogcheon metamorphic belts (II) (On the metamorphism and metamorphic facies of Gyeonggi massif). Jour. Geol. Soc. Korea 15: p. 67-88.

Na, K.C. (1979b) Regional metamorphism in the

Gyeonggi Massif with comparative studies on the Yeoncheon and Ogcheon metamorphic belts(III) (Comparative studies on Gyeonggi, Yeoncheon, and Ogcheon metamorphic belts). Jour. Geol. Soc. Korea 15 : p. 127 – 133.

Nash, J.T. (1972) Fluid inclusion studies of some gold deposits in Nevada. U.S. Geol. Surv. Prof. Paper 800 – C : p. 15 – 19.

Ohmoto, H., Rye, R.O. (1979) Isotopes of sulfur and carbon. In : Barnes H.L. (ed.), Geochemistry of Hydrothermal Ore Deposits, Second Ed., Wiley and Sons, New York, p. 509 – 567.

O'Neil, J.R., Clayton, R.N., Mayeda, T.K. (1969) Oxygen isotope fractionation in divalent metal carbonates. Jour. Chem. Phys. 51 : p. 5547 – 5558.

Potter, R.W. III, Clynne, M.A., Brown, D.L. (1978) Freezing point depression of aqueous sodium chloride solutions. Econ. Geol. 73 : p. 284—285.

Roedder, E. (1984a) Fluid inclusions. Reviews in Mineralogy 12 : 644 p.

Roedder, E. (1984b) Fluid – inclusion evidence bearing on the environments of gold deposition. In : Foster, R.p. (ed.), Gold 82 : The Geology, Geochemistry and Genesis of Gold Deposits, Geol. Soc. Zimbabwe Spec. Pub. 1 : p. 129 – 163.

Roedder, E., Ingram, B., Hall, W.E. (1963) Studies of fluid inclusions. III. Extraction and quantitative analysis of inclusions in the milligram range. Econ. Geol. 58, p. 353 – 374.

Rye, R.O. (1966) The carbon, hydrogen, and oxygen isotopic compositions of hydrothermal fluids responsible for the lead – zinc deposits at Providencia, Zacatecas, Mexico. Econ. Geol. 61 : p. 1339 – 1427.

Sakai, H. (1968) Isotopic properties of sulfur compounds in hydrothermal processes. Geochem. Jour. 2 : p. 29 – 49.

Seward, T.M. (1984) The transport and deposition of gold in hydrothermal systems. In : Foster, R.P. (ed.), Gold 82 : The Geology, Geochemistry and Genesis of Gold Deposits, Geol. Soc. Zimbabwe Spec. Pub. 1 : p. 165 – 181.

Shelton, K.L.(1983) Composition and origin of ore – forming fluids in a carbonate – hosted porphyry copper and skarn deposit : A fluid inclusion and stable isotopic study of Mines Gaspe, Quebec. Econ. Geol. 78 : 387 – 421.

So, C.S. Chi, S.J., Shelton, K.L. (1987a) Stable isotope and fluid inclusion studies of gold – silver – bearing vein deposits, Cheonan – Cheongyang – Nonsan mining district, Republic of Korea : Nonsan area. Neues Jb. Min. Abh 158:p.47 – 65.

So, C.S., Chi, S.J., Yu, J.S., Shelton, K.L. (1987b) The Jeonui gold – silver mine, Republic of Korea : A geochemical study. Mining Geol. (Japan) 37 : p.313 – 322.

So, C.S., Choi, S.H., Chi, S.J. (1987c) Genetic environments of the Geumryong gold – silver deposit, Jur. Geol. Soc. Korea 23 : p. 321 – 330.

So, C.S., Shelton, K.L. (1987a) Stable isotope and fluid inclusion studies of gold – silver – bearing hydrothermal vein deposits, Cheonan – Cheongyang – Nonsan mining district, Republic of Korea : Cheonan area. Econ. Geol 82 : p. 987 – 1000

So, C.S., Shelton, K.L. (1987b) Fluid inclusion and stable isotope studies of gold – silver – bearing hydrothermal vein deposits, Yeoju mining district, Republic of Korea. Econ. Geol. 82 : p. 1307 – 1318.

Sourirajan, S., Kennedy, G.C. (1962) The system H_2O – NaCl at elevated temperatures and pressures. Am. Jour. Sci. 260 : p. 115 – 141.

Taylor, H.P. Jr. (1974) The application of oxygen and hydrogen isotope studies to problems of hydrothermal alteration and deposition. Econ. Geol. 69 : p. 843 – 883.

Tsusue, A., Mizuta, T., Watanabe, M., Min, K.G. (1981) Jurassic and Cretaceous granitic rocks in South Korea. Mining Geol. (Japan) 31 : p. 1261 – 1280.

한반도 열수 금광상의 지화학적 연구 : 양평-원주지역 광화대

소칠섭 · 최상훈 · 이경용 · Shelton, Kevin L.

요약 : 양평-원주지역 광화대에는 원생대 편마암류 내에 NS 단층파쇄대를 충진한 수십개조의 평행한 함 금-은 열수 맥상 광상들이 부존한다. 구조운동에 수반되어 3회에 걸쳐 진행된 열수 광화작용의 시기는 67.5±1.6m.y.이다. 일렉트럼(55.0-60.0wt.% Au)-방연석-섬아연석의 광화정출 작용은, 최대 압력 50기압 하에서, 8.2-2.9wt.% NaCl상당 염농도를 갖는 광화유체로부터 260-180℃에 걸쳐서 비등작용과 함께 냉각 작용에 의하여 진행되었다. 비등작용과 유화광물의 침전에 의한 광화유체내 H_2S의 감소는 유황동위원소의 re-equilibration을 야기하고 H_2S의 $\delta^{34}S$값을 광화초기 −1.4-2.7‰에서 후기 6.6-9.2‰로 증가시켰다. 광화작용이 진행됨에 따라 열수유체내의 산소, 수소 안정동위원소의 값은 점점 감소하여 천수의 값에 가까와지는데, 이는 천수의 유입이 점진적으로 증가하였음을 뜻하며, 쥬라기 심부 열수계보다 큰 water-rock interaction의 값을 갖는 백악기 천부 열수 광상들의 값과 일치한다.